

# Cyclic voltammetric studies of pasted nickel hydroxide electrode microencapsulated by cobalt

X. Y. WANG, J. YAN, Y. S. ZHANG, H. T. YUAN, D. Y. SONG

*Institute of New Energy Material Chemistry, Nankai University, Tianjin 300071, China*

Received 22 May 1997; accepted in revised form 3 March 1998

Spherical nickel hydroxide microencapsulated by cobalt has been used as the electrochemically active material in pasted-type nickel electrodes of rechargeable alkaline batteries. Cobalt coating on the surface of nickel hydroxide particles can be converted to CoOOH during charge. Well distributed CoOOH forms the conductive network on the surface of nickel hydroxide particles, thereby leading to higher utilization of active material. Cyclic voltammetric studies suggest that nickel hydroxide microencapsulated by cobalt has better reversibility of the Ni(OH)<sub>2</sub>/NiOOH redox couple, greater discharge capacity and higher oxygen evolution overpotential than nickel hydroxide with added cobalt metal powder as a conductor. The mechanism of the electrode reaction is still found to be controlled by proton diffusion, and the proton diffusion coefficient is  $1.2 \times 10^{-9} \text{ cm}^2 \text{ s}^{-1}$ .

Keywords: *cyclic voltammetry, microencapsulation, nickel hydroxide electrode, oxygen evolution overpotential, proton diffusion coefficient, reversibility*

## 1. Introduction

The electrochemical properties of the nickel hydroxide electrode has been the subject of investigation for several decades, due to its application as the positive plate in Ni–Cd, Ni–H<sub>2</sub> and Ni–metal hydride (MH) batteries [1–3]. The effect of cobalt hydroxide as a performance enhancing additive on the nickel hydroxide electrode has been known for some time [4]. It is generally believed that the presence of cobalt is responsible for reducing the oxygen evolution overpotential and improving the performance of the nickel hydroxide electrode [5–7].

It is known that, after initial oxidation, cobalt remains in the (III) state throughout its cycle life within a nickel hydroxide lattice and that, as a result, it does not contribute through the Co(II)/Co(III) couple to the capacity of the electrode [5]. However, cobalt, being an element of a variable valence, is considered to increase the proton conductivity of nickel hydroxide [8] thereby improving electrode performance. In general, cobalt coexists in the lattice of nickel hydroxide in the form of cobalt hydroxide by chemical impregnation or electrochemical impregnation. Nevertheless, the distribution of cobalt is nonuniform. Uneven distribution of cobalt within the active material–nickel hydroxide may play a diminished role during activation of the active material and, as a consequence, the active material cannot be fully utilized in practical electrodes. Recently, in order to further increase the energy density of Ni–Cd and Ni–MH batteries, a low cost and high performance pasted nickel electrode made from a porous foam nickel or fibrous nickel substrate has been developed. Since active material–nickel hydroxide is a

low conductivity p-type semiconductor [9], there is a relatively large resistance between the nickel hydroxide particles and the current collector, thus resulting in poor electrode performance and a relatively low active material utilization. To reduce the resistance between the active material and current collector, and to maximize electrode performance, many researchers add increased quantities of cobalt to their electrodes. The addition of cobalt in relatively large amounts, however, results in a substantial decrease in the discharge potential plateau and an increase in cost.

In our previous studies, electroless cobalt on the surface of spherical nickel hydroxide particles has been developed [10, 11]. In the present study, we investigate the electrochemical characteristics of the nickel hydroxide electrode microencapsulated with cobalt by cyclic voltammetry, and the reversibility of the Ni(OH)<sub>2</sub>/NiOOH redox reaction and the oxygen evolution overpotential. In addition, we also discuss the reasons for the high performance of nickel hydroxide electrodes microencapsulated by cobalt.

## 2. Experimental details

Spherical nickel hydroxide was prepared by reactive crystallization under highly controlled pH conditions using NiSO<sub>4</sub> and NaOH solutions in addition to aqueous ammonia as a complexing agent and CoSO<sub>4</sub> as an additive. The sample was β-Ni(OH)<sub>2</sub> and contained about 1.5 wt % cobalt in the form of cobalt hydroxide in its lattice as indicated by XRD measurements and chemical analysis. Electroless cobalt deposition was carried out in a solution containing cobalt sulfate, sodium citrate, ammonium sulfate and

sodium hypophosphite [10]. Scanning electron micrographs of the spherical nickel hydroxide particles before and after electroless cobalt are shown in Fig. 1. If the SEM of a spherical particle microencapsulated by cobalt in Fig. 1(b) is enlarged, it can be distinctly seen that surface roughness of nickel hydroxide particle increases, thus indicating that the particle has a large real surface area [11].

Nickel foam (1 cm × 1 cm) was used as the nickel electrode substrate. Two kinds of pasted-type electrodes were prepared as follows:

*Electrode A:* The spherical nickel hydroxide particles microencapsulated by 5 wt % cobalt were mixed with an appropriate amount of 1 wt % polytetrafluoroethylene (PTFE) aqueous suspension (60%) and kneaded to obtain paste. The paste was incorporated into the nickel foam substrate using a spatula, dried at 60 °C for 1 h, and then pressed at 20 MPa for 1 min. to assure good electrical contact between the substrate and the active material.

*Electrode B:* The spherical nickel hydroxide particles and cobalt metal particles which was 5% of the total

weight of the active material, were uniformly mixed in an agate mortar. Then appropriate amount of 1 wt % PTFE aqueous suspension was added and kneaded to obtain a paste. Subsequent procedures were the same as for Electrode A.

All cyclic voltammetric studies were performed in a three-compartment electrolysis cell at 25 °C using an EG&G PARC model 273 potentiostat/galvanostat and M270 electrochemical analysing system with a personal computer. The electrolyte consisted of 6 M KOH + 0.6 M LiOH. Two nickel sheet counterelectrodes were placed at the side and the working electrode was positioned in the center. A Hg/HgO reference electrode was used with a luggin capillary in the region of the working electrode. The working electrodes were activated by charge/discharge cycling prior to the experiments.

### 3. Results and discussion

Figure 2 shows the cyclic voltammograms of electrodes A and B. Only one anodic oxidation peak for Electrode A, appearing at about 500 mV, was recorded prior to oxygen evolution. Similarly, only one oxyhydroxide reduction peak at about 240 mV was observed on the reverse sweep. Similar voltammograms were also observed for electrode B, with added cobalt metal powder, but the anodic peak corresponding to nickel hydroxide oxidation shifts to a more positive potential, and the cathodic peak potential corresponding to nickel oxyhydroxide reduction shifts to a less positive potential, compared to that of electrode A. This is in agreement with other researchers [1, 2, 5, 7] who incorporated Co into the lattice of nickel hydroxide in the form of  $\text{Co}(\text{OH})_2$ .

It may also be noted from Fig. 2 that no detectable oxidation peak for cobalt was observed although 5 wt % cobalt had been microencapsulated on the surface of the nickel hydroxide particles (electrode A) and 5 wt % cobalt metal powder had been added as a conductor (electrode B). The absence of an oxidation peak for cobalt in the voltammograms of nickel hydroxide has been previously reported [1, 5, 10]. In the present study the probable cause of this phenomenon is the fact that the cobalt coating or cobalt metal powder is oxidized to cobalt oxyhydroxide when initial activation is carried out using constant current charge/discharge cycling prior to the experiments, while this oxidation reaction is irreversible [5].

To compare the characteristics of the electrodes, the results of the cyclic voltammetric study in Fig. 2 are tabulated in Table 1. The average peak potential,  $E_{\text{rev}}$ , is taken as an estimate of the reversible potential and the difference in the anodic and cathodic positions,  $\Delta E_{\text{a,c}}$ , is taken as an estimate of the reversibility of the redox reaction [7, 12]. Oxygen evolution is a parasitic reaction during charging of nickel battery electrodes. McKubre [13] showed that the reversible potential for oxygen evolution is more negative than that for  $\text{Ni}(\text{OH})_2/\text{NiOOH}$ . To compare the effects of two kinds of electrode on the oxygen evolution

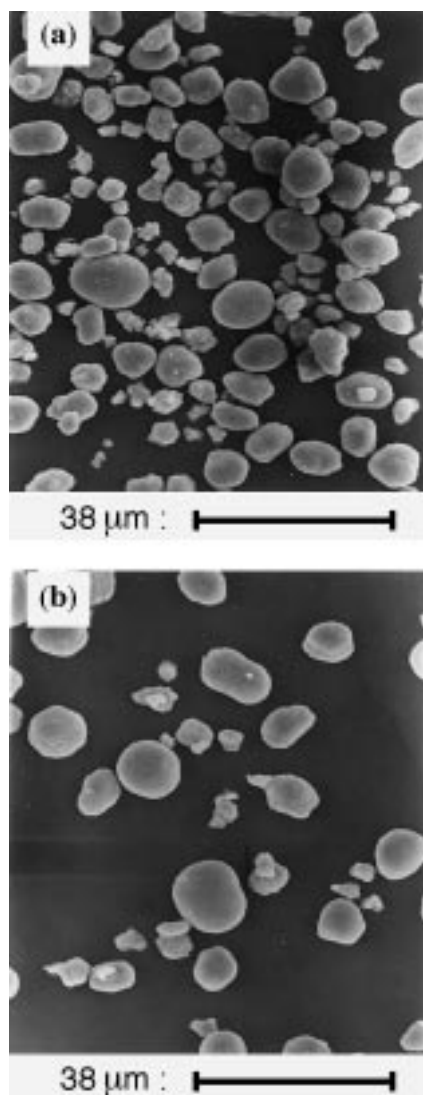


Fig. 1. SEM photographs of spherical nickel hydroxide: (a) before microencapsulated cobalt; (b) after microencapsulated cobalt.

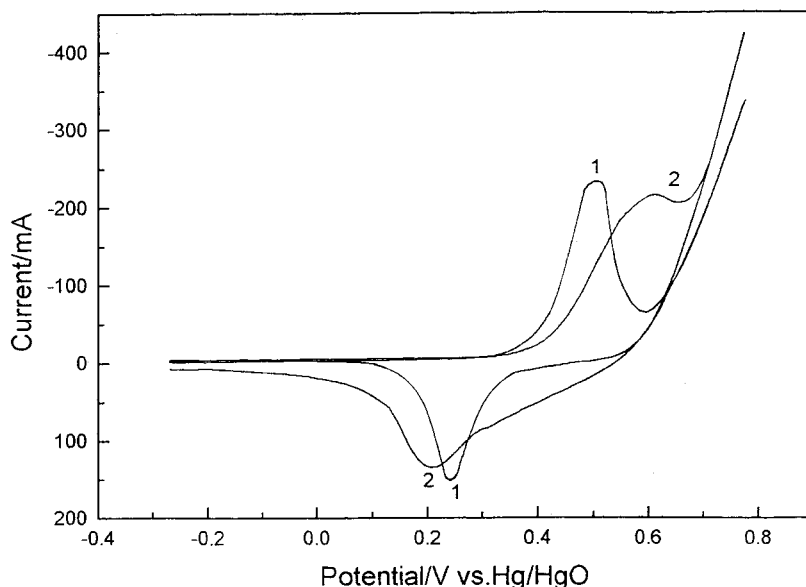


Fig. 2. Cyclic voltammograms of different electrodes: (1) electrode A, (2) electrode B. Scan rate 1 mV s<sup>-1</sup>.

reaction, the overpotential at 150 mA was estimated from voltammograms. For this, it was assumed that the return sweep provided the best approximation of the steady-state condition, since there would be less interference from the nickel hydroxide redox reaction [10]. Thus, the overpotential was taken as the potential on the return sweep required to produce 150 mA of anodic current minus the reversible oxygen potential (taken as 303 mV vs Hg/HgO [12]).

The results in Fig. 2 and Table 1 illustrate that the presence of cobalt coating on the surface of nickel hydroxide particles (electrode A) allows the electrode to charge at a significantly less positive potential (510 mV instead of 620 mV vs Hg/HgO). In addition, the charge process appears to occur more reversibly in the presence of cobalt coating (electrode A) than in its absence (electrode B) ( $\Delta E_p$  is 270 mV instead of 418 mV). Moreover, oxygen evolution appears to be more difficult for electrode A than electrode B. The oxygen evolution overpotential shifts to a more positive value in the presence of cobalt coating (electrode A) (397 mV instead of 357 mV). It can also be seen from Fig. 2 that the anodic charge and peak current associated with nickel hydroxide oxidation for electrode A increase considerably, while the cathodic peak current and the associated cathodic charge were difficult to determine, since the cathodic current base line was obscured by the oxygen evolution current.

Table 1. Results of cyclic voltammetry experimental for different electrodes

Electrode	$E_{anodic}$ /mV	$E_{cathodic}$ /mV	$\Delta E_{a,c}$ /mV	Oxygen evolution overpotential /mV
A	510	240	270	397
B	620	202	418	357

However, it can be qualitatively seen from Fig. 2 that the cathodic charge and peak current for electrode A is higher than those for electrode B. Thus, these indicate clearly that nickel hydroxide electrode micro-encapsulated by cobalt allows the charge process to occur more easily and more reversibly, suggesting that much more active material can be utilized on the electrode surface during charge. Besides, due to the increase in the oxygen evolution overpotential and the decrease of the oxidation peak potential of nickel hydroxide for electrode A, the nickel hydroxide can be allowed to be oxidized fully during charge, and the nickel oxyhydroxide can be reduced completely during discharge, implying that electrode A has a greater discharge capacity and can give a higher utilization of active material. Furthermore, the increase in oxygen evolution overpotential is undoubtedly beneficial in lowering the internal pressure of the battery.

Typical cyclic voltammograms for nickel hydroxide (electrode A) microencapsulated by cobalt at various scan rates are shown in Fig. 3. As scan rate increases, anodic peak potential and cathodic peak potential shift in the more anodic and more cathodic direction, respectively. Characteristic cyclic voltammetry parameters obtained from Fig. 3 are shown in Fig. 4 as a function of sweep rate. The cyclic voltammetric peak currents  $i_{pa}$  against  $V^{1/2}$  plot, where  $V$  is the voltage scan rate, gives a reasonable linear relationship, while  $i_{pa}$  against  $V$  does not give a linear relationship. In semiinfinite diffusion controlled cyclic voltammetry in liquid electrolytes,  $i_{pa}$  against  $V^{1/2}$  gives a linear relationship regardless of scan rate for a kinetically uncomplicated redox reaction; for an adsorption process,  $i_{pa}$  against  $V$  is expected to be linear at different rates. In the present study, the linear relationship between  $i_{pa}$  and  $V^{1/2}$  suggests that the oxidation of nickel hydroxide is diffusion limited, as noted by other authors [15, 16].

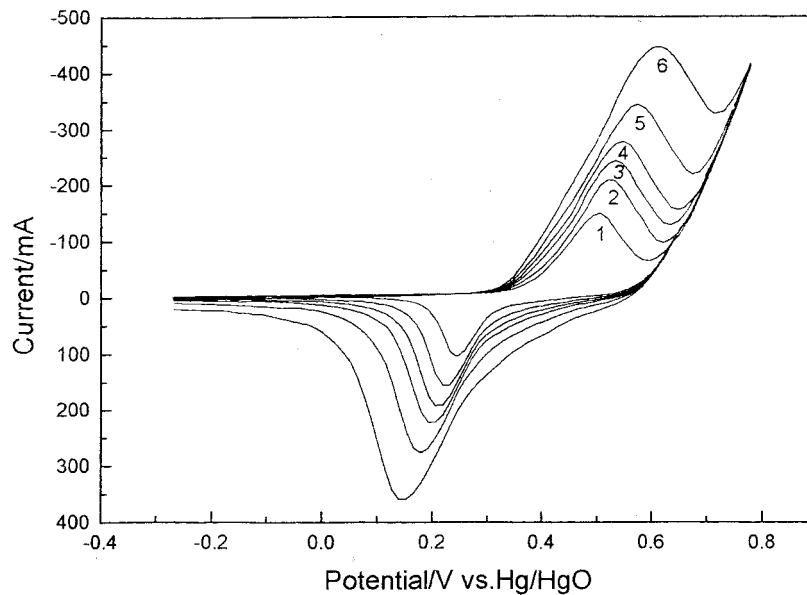
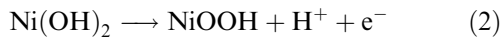


Fig. 3. Cyclic voltammograms of electrode A at various scan rates: (1) 0.5, (2) 1, (3) 2, (4) 4, (5) 6 and (6) 10  $\text{mV s}^{-1}$ .

In the case of semiinfinite diffusion, the peak current  $i_p$  may be expressed by the classical Sevcik equation [14]:

$$i_p = 2.69 \times 10^5 n^{3/2} A D_o^{1/2} V^{1/2} C_o \quad (1)$$

Here,  $n$  is the number of electrons transferred,  $A$  is the apparent surface area of the electrode,  $D_o$  is the diffusion coefficient of the rate limiting species, that is, proton, and  $C_o$  is the proton concentration. To estimate the proton concentration in the nickel hydroxide, we assumed it to be the same as that of  $\text{Ni(OH)}_2$  from the stoichiometry of reaction [17]:



The concentration of  $\text{Ni(OH)}_2$  is estimated by dividing the molecular weight of  $\beta\text{-Ni(OH)}_2$  by its density,  $3.97 \text{ g cm}^{-3}$  [18]. According to Equation 1 and the

slope of  $i_{pa}$  against  $V^{1/2}$  in Fig. 4, we calculate that the proton diffusion coefficient in nickel hydroxide is  $1.2 \times 10^{-9} \text{ cm}^2 \text{ s}^{-1}$ . Zhang *et al.* [17] reported a diffusion coefficient of  $1.0 \times 10^{-11} \text{ cm}^2 \text{ s}^{-1}$  for  $\beta\text{-Ni(OH)}_2$  from cyclic voltammetry. This value is considerably smaller than the present value. This difference may be ascribed to both the preparation of the electrode and the presence of the cobalt coating on the surface of the nickel hydroxide. The electrode used by Zhang *et al.* [17] was prepared by impregnation, whereas the present electrode is pasted. The presence of cobalt on the surface of nickel hydroxide can increase the proton and electron conductivity of nickel hydroxide [8, 11] and thus give a relatively large proton diffusion coefficient.

The potentials of the current peaks in Fig. 3 change linearly with  $\log V$  (Fig. 5), which has also

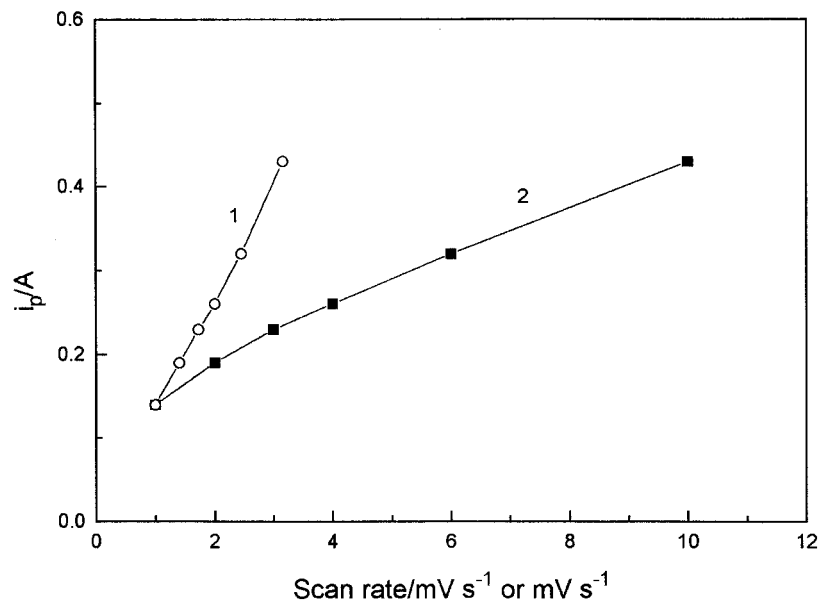


Fig. 4. Variation of anodic peak current with scan rate for electrode A. (1)  $i_p-V^{1/2}$ , (2)  $i_p-V$ .

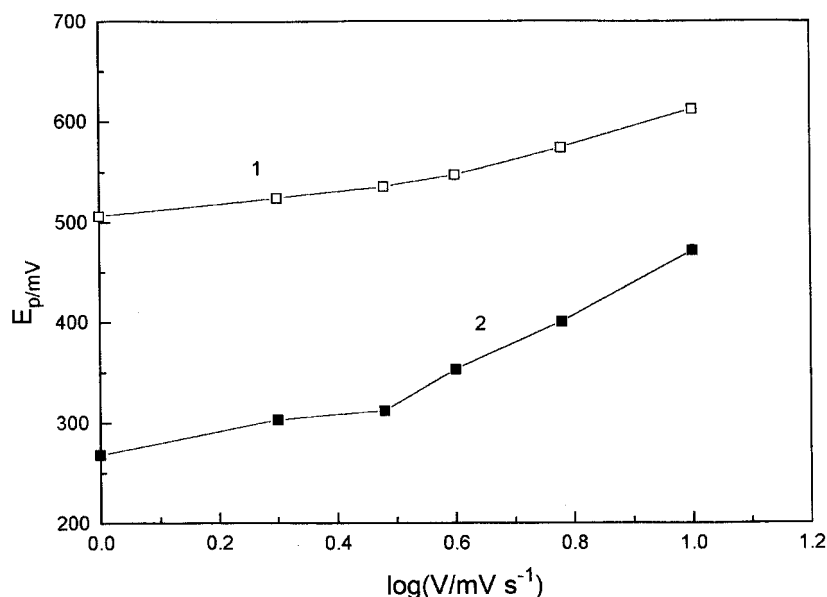
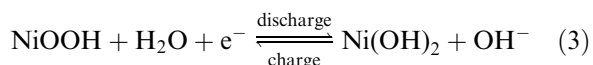


Fig. 5. Variation of  $E_{pa}$  and  $\Delta E_p$  with scan rate for electrode A. (1)  $E_p - \log V$ , (2)  $\Delta E_p - \log V$ .

been observed by Guzman [16]. But as seen from Fig. 5, the magnitude of the change is very small, indicating that the same process is taking place at all scan rates [4]. The difference ( $\Delta E$ ) between  $E_{pa}$  and  $E_{pc}$  is fairly constant at low scan rates, and generally increases at high scan rate. Thus, on the basis of liquid electrolyte reversibility criteria, the reaction approaches reversibility only at low scan rates [4]. Of course, since no attempt was made at  $iR$  compensation, increases of  $\Delta E_p$  observed at higher scan rates may be due to greater uncorrected potential differences at higher scan current. However, as a general rule, the nickel hydroxide electrode microencapsulated by cobalt has the same kinetic mechanism as the nickel hydroxide electrodes incorporating cobalt by chemical or electrochemical methods. Hence, the existence of a cobalt coating at the surface of nickel hydroxide does not change the kinetic mechanism for  $Ni(OH)_2/NiOOH$  redox reaction, but does improve the electrode performance, that is, it increases the discharge capacity of the electrode, improves the reversibility of the electrode, enhances the utilization of the active material and increase the oxygen evolution overpotential.

The redox reaction taking place at nickel hydroxide during discharge and charge can be represented as



It has been considered that during discharge a proton diffuses from the film/electrolyte interface into the active material and an electron enters across the conducting substrate/film interface. During charge the proton diffuses to the film/electrolyte interface to react with a hydroxyl ion to form water [19]. Barnard [20] has proposed a homogenous charge-heterogeneous discharge mode, and considered that the high-charged phase is a n-type semiconductor and the low-charge one is an electronic insulator or a low

conductivity p-type semiconductor. Therefore, during discharge, as a result of the low electronic conductivity of the reduced phase, nickel (II) species accumulate at the hydroxide/electrolyte and form an insulative boundary layer between the current collector and the active material. This layer prevents discharge of the crystallite core. Hence, it is difficult for nickel (III) species which form during charge to revert to the completely reduced material, and thus the oxidation states of the pasted nickel electrode remains relatively high even at the end of discharge and the utilization of the active material is relatively low. However, after the surface of nickel hydroxide is microencapsulated by cobalt coating, cobalt can be oxidized to cobalt oxyhydroxide during charge, which henceforth remains as cobalt oxyhydroxide because of the irreversibility of the  $Co(II)/Co(III)$  couple. Well distributed cobalt oxyhydroxide is highly conductive and is expected to provide continuity of a good electrical path between the active material and the substrate. Besides, cobalt, being an element with a variable valence, improves the proton conductivity of the nickel hydroxide. Thus the proton diffusion coefficient is higher than those reported by other authors. Accordingly, the presence of  $Co(III)$  at the surface of nickel hydroxide maintains the current path allowing more complete discharge of the core material.

Both the anodic peak currents and anodic charge were found to increase for electrode A in comparison to electrode B (Fig. 2). Qualitatively, cathodic peak currents and the associated cathodic charge also increased. This indicates that the utilization of microencapsulated active material is improved. But, it is well known that the higher utilization of active material is correlated with the uniform surface distribution of cobalt.

For electrode B, although 5 wt % cobalt metal powder was added as a conductor, the distribution of

cobalt metal powder at the surface of nickel hydroxide particles was in the form of islands and was nonuniform. In contrast, for electrode A, the cobalt coating was uniform and formed a well-distributed CoOOH conductive network. Therefore, electrode A has the higher active material utilization and the better electrode performance.

#### 4. Conclusion

(i) Nickel hydroxide electrodes microencapsulated by cobalt show better reversibility of the Ni(OH)<sub>2</sub>/NiOOH redox reaction, greater discharge capacity and higher oxygen evolution overpotential than nickel hydroxide electrodes treated by addition of cobalt metal powder as a conductor.

(ii) The cobalt coating can be oxidized into highly conductive CoOOH and form a well-spread CoOOH conductive network at the surface of the spherical nickel hydroxide particles during charge to provide a good electrical connection between the active material and the substrate, thus improving utilization of active material.

(iii) The presence of a cobalt coating on the nickel hydroxide surface does not change the kinetic mechanism of the electrode reaction and modifies proton conductivity of the nickel hydroxide. The electrode reaction is still found to be controlled by proton diffusion and the proton diffusion coefficient is  $1.2 \times 10^{-9} \text{ cm}^2 \text{ s}^{-1}$ .

#### Acknowledgement

This project was granted financial support from China Postdoctoral Science Foundation.

#### References

- [1] A. K. Sood, *J. Appl. Electrochem.* **16** (1986) 274.
- [2] M. E. Unates, M. E. Folquer, J. R. Vilche and A. J. Arvia, *J. Electrochem. Soc.* **139** (1992) 2697.
- [3] Y. J. Kim, S. Srinivasan and A. J. Appleby, *J. Appl. Electrochem.* **20** (1990) 377.
- [4] D. F. Pickett and J. T. Maloy, *J. Electrochem. Soc.* **125** (1978) 1026.
- [5] R. D. Armstrong, G. W. D. Briggs and E. A. Charles, *J. Appl. Electrochem.* **18** (1988) 215.
- [6] A. Visintin, A. Anani, S. Srinivasan and A. J. Appleby, L. Donaghe and H. S. Lim, *J. Power Source* **51** (1994) 433.
- [7] P. V. Kamath and M. F. Ahmed, *J. Appl. Electrochem.* **23** (1993) 225.
- [8] M. Oshitani, Y. Sasaki and K. Takashima, *J. Power Source* **12** (1984) 219.
- [9] R. Barnard, G. T. Crickmore, J. A. Lee and F. L. Tye, *J. Appl. Electrochem.* **10** (1981) 61.
- [10] Y. S. Zhang, X. Y. Wang, J. Yan, Z. Zhou, H. T. Yuan and D. Y. Song, *Chinese Patent Appl.* 97 111 331. 9 (1997).
- [11] X. Y. Wang, J. Yan, Y. S. Zhang, Z. Zhou, H. T. Yuan and D. Y. Song, *J. Power Sources*, (in press)
- [12] D. A. Corrigan and R. M. Bendert, *J. Electrochem. Soc.* **136** (1989) 723.
- [13] M. C. H. McKubre and D. D. Macdonald, *J. Energy* **5** (1981) 368.
- [14] Southampton Electrochemistry Group, 'Instrumental Methods in Electrochemistry', 178, Ellis Horwood, England (1985).
- [15] D. M. MacArthur, *J. Electrochem. Soc.* **117** (1970) 729.
- [16] R. S. S. Guzman, J. R. Vilche and A. J. Arvia, *ibid.* **125** (1978) 1578.
- [17] C. Zhang and S. M. Park, *ibid.* **134** (1987) 2966.
- [18] M. Oshitani, T. Takayama, K. Takashima and S. Tsuji, *J. Appl. Electrochem.* **16** (1986) 403.
- [19] A. H. Zimmeman and P. K. Effa, *J. Electrochem. Soc.* **131** (1984) 709.
- [20] R. Barnard, C. F. Randell and F. L. Tye, *J. Appl. Electrochem.* **10** (1980) 109.